# Poly(Ethylene Glycol)-Alendronate Coated Nanoparticles for Magnetic Resonance Imaging of Lymph Nodes

Sofia Bisso[a], Anna Degrassi[b], Davide Brambilla[a,c] and Jean-Christophe Leroux[a*]

[a]*Institute of Pharmaceutical Sciences, Department of Chemistry and Applied Biosciences, ETH Zurich, Zurich, Switzerland.*

[b]*Biology Department, Nerviano Medical Sciences s.r.l., Nerviano (MI), Italy.*

[c]*Faculté de Pharmacie, Université de Montréal, Montréal, QC, Canada.*

Supporting Information

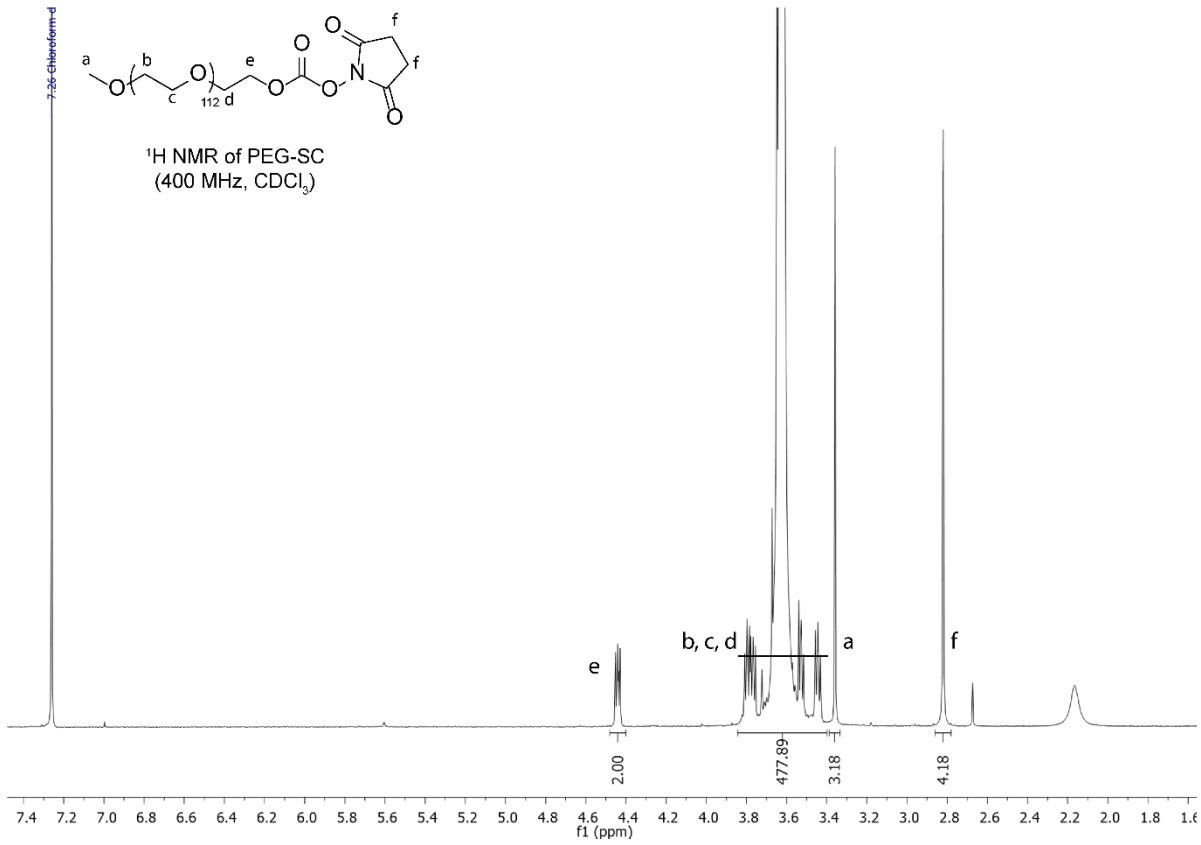


**Figure S1.** $^{1}H$ NMR spectrum in $CDCl_3$ of the intermediate derivative PEG-SC.

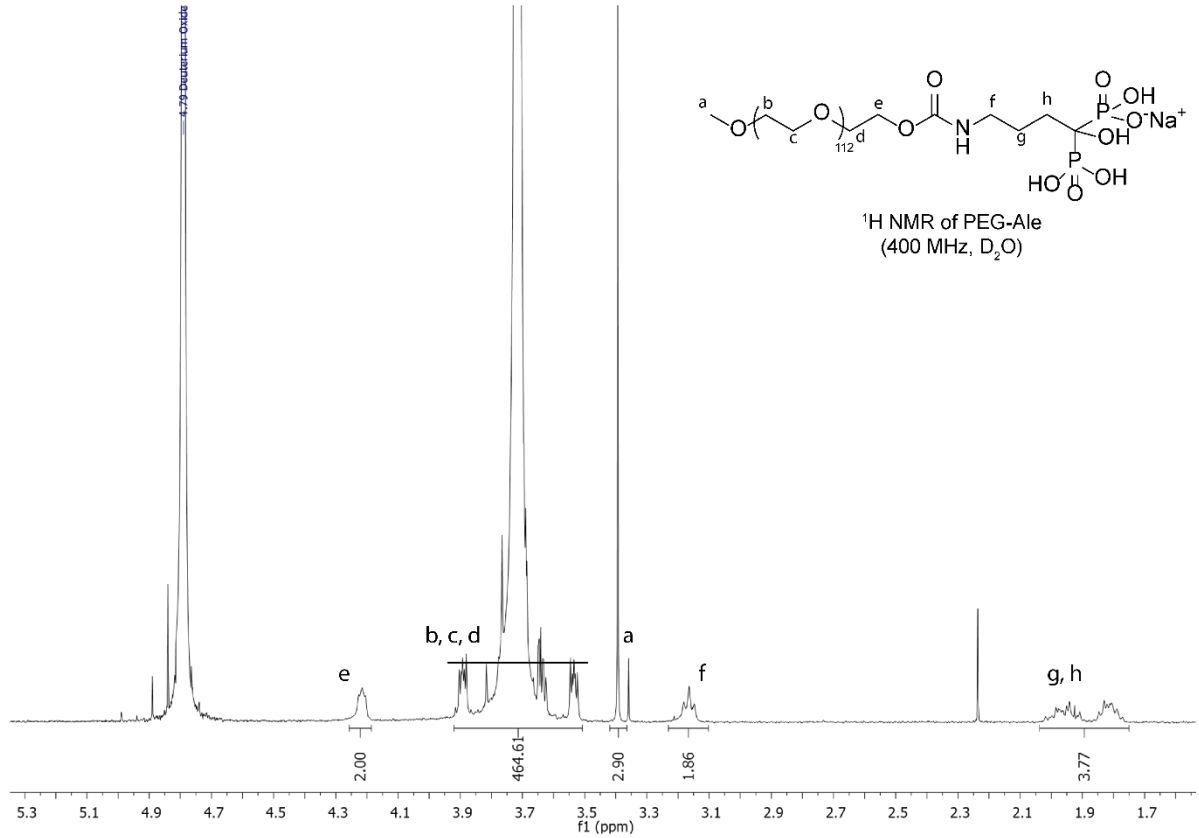


**Figure S2.** $^1$H NMR spectrum in $D_2O$ of PEG-Ale.

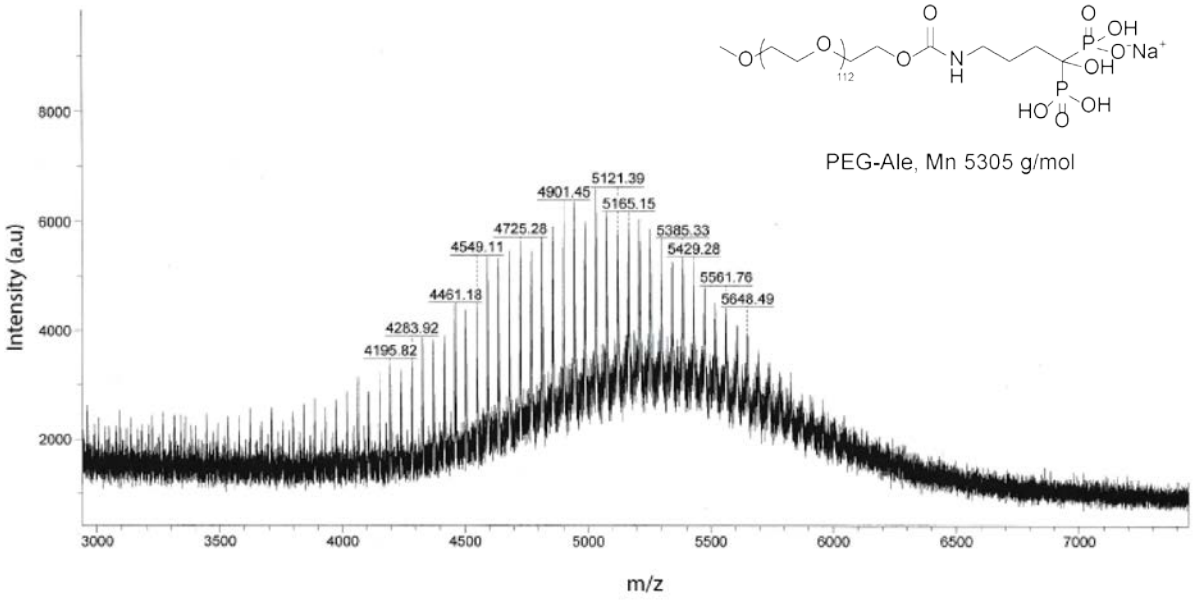


**Figure S3.** Mass spectrum of PEG-Ale.

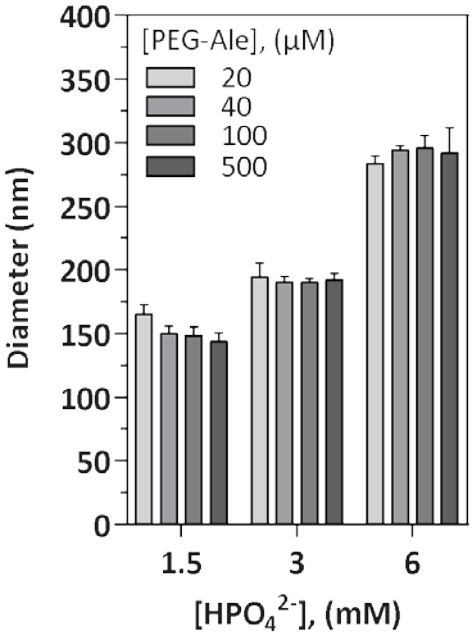


**Figure S4.** Size of Gd-DTPA/CaP NPs prepared with 1.5 – 6 mM [$HPO_4^{2-}$], 250 mM [$CaCl_2$]; and 20-500 μM [PEG-Ale]. Data are presented as mean + SD (n = 3).

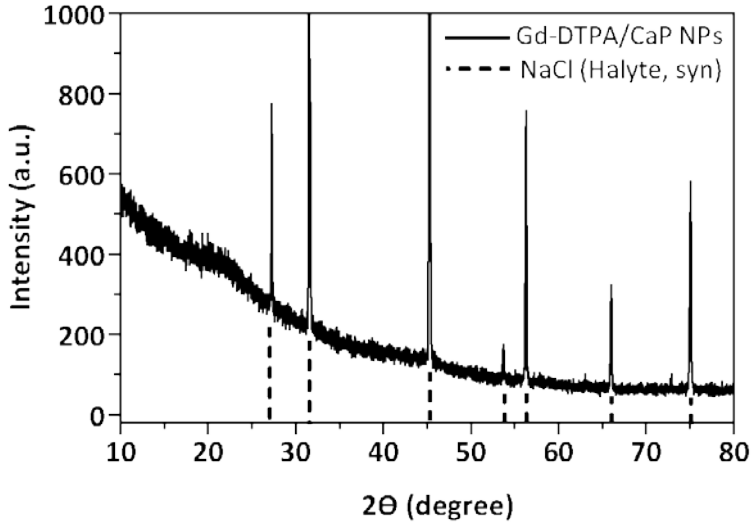


**Figure S5.** XRD pattern of Gd-DTPA/CaP NPs. All the peaks belong to NaCl, which was present in the preparation buffer of the particles; no characteristic peaks of crystalline hydroxyapatite were observed.

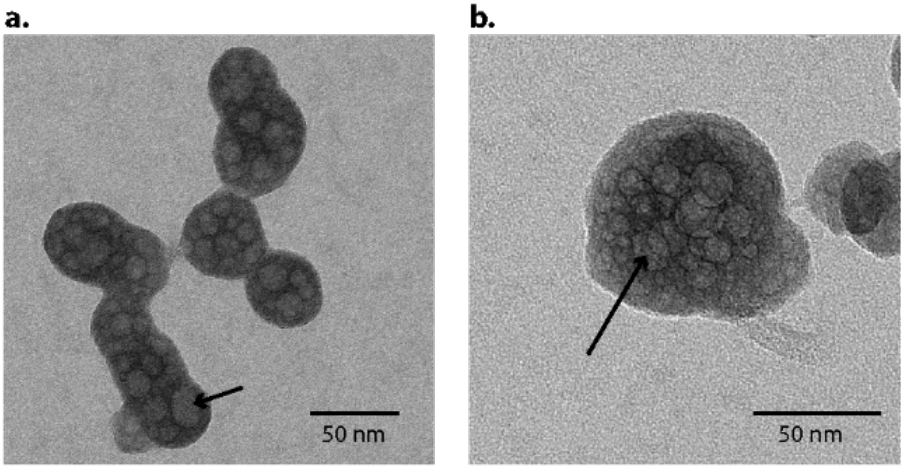


**Figure S6.** TEM micrograph of purified Gd-DTPA/CaP NPs. Aggregates of a small number of spheroidal particles were observed (a). A single Gd-DTPA/CaP particle showing the typical internal porosity of amorphous CaP (b). Arrows indicate porosity in the particle structure.

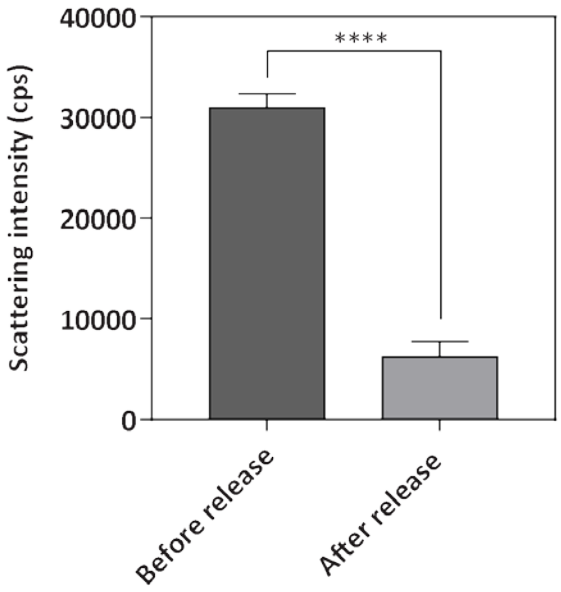


**Figure S7.** Scattering intensity (cps) of Gd-DTPA/CaP NPs measured by DLS before and after completion of the release study. The decrease in scattering intensity after 24 h dialysis at 37 °C is likely associated to the dissolution of the particles. All the measurements were performed using a fixed attenuation of 5%. Mean + SD (n = 3), ****$p < 0.0001$.

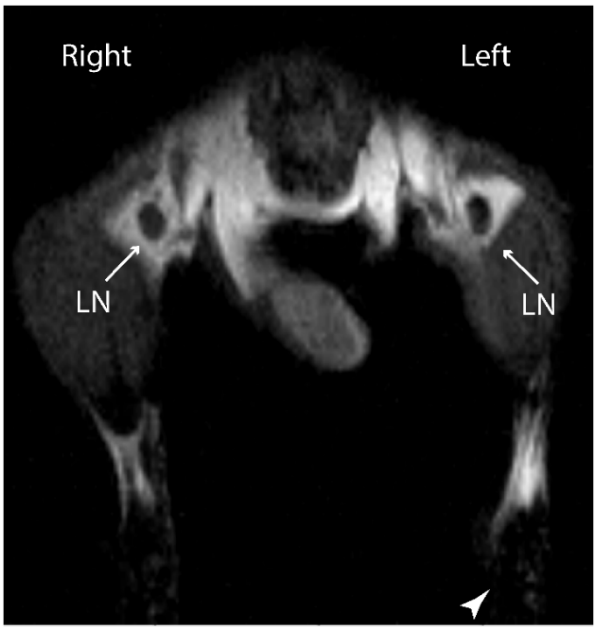


**Figure S8.** Full FOV of coronal precontrast slice showing the position of the right and left popliteal LNs. Injections of the tracers were performed in the forelimb of the left foot (as indicated with the arrowhead).

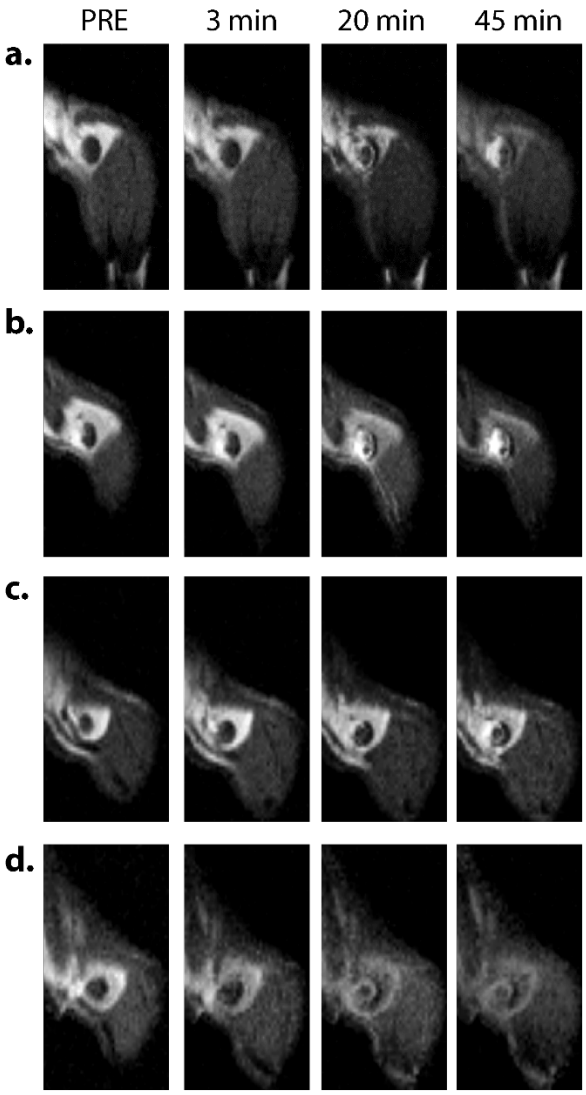


**Figure S9.** MRI images after foot paw administration of Gd-DTPA/CaP NPs show slow deposition rate in the LN and small variability in the onset and localization of the signal. Precontrast and postcontrast acquisitions of four independent experiments (a, b, c and d) are displayed. Gd-DTPA/CaP NPs accumulated along the margins and in the medial part of the LN starting from 20 min after injection.

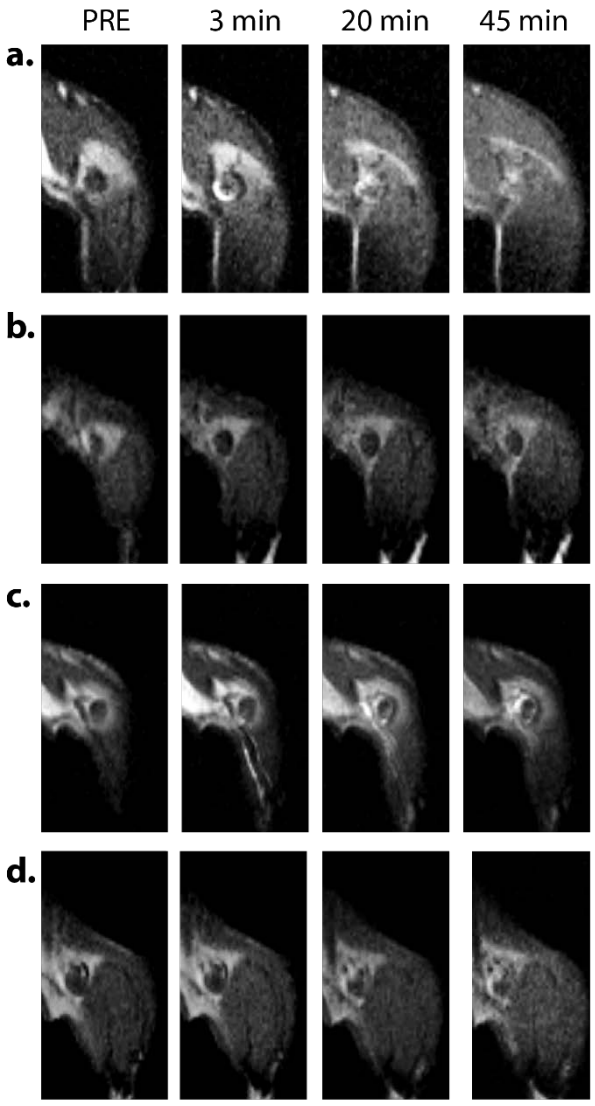


**Figure S10.** MRI images show high variability in contrast enhancement upon foot paw administration of gadobutrol. Precontrast and postcontrast acquisitions of four independent experiments (a, b, c and d) are displayed. In (a) the tracer quickly deposited along the margins of the LN and in the region of the subcapsular sinuses, respectively. In three other mice, a low amount (c and d) or no gadobutrol (b) was found in the LN, and different kinetics of deposition were observed.

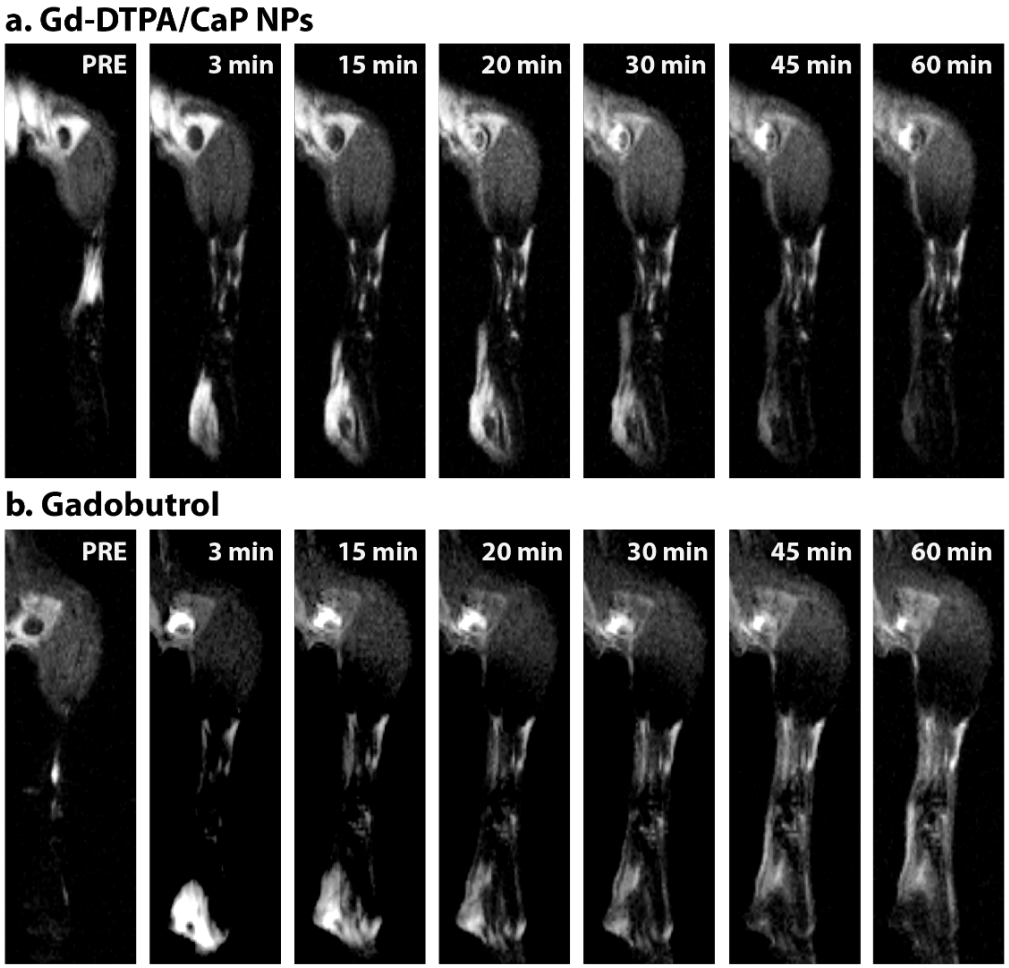


**Figure S11.** MRI images shows that after foot paw administration of Gd-DTPA/CaP NPs (a) or gadobutrol (b), a progressive decrease in the MRI at the injection site correlates with accumulation of the tracers in the ipsilateral draining popliteal LN.

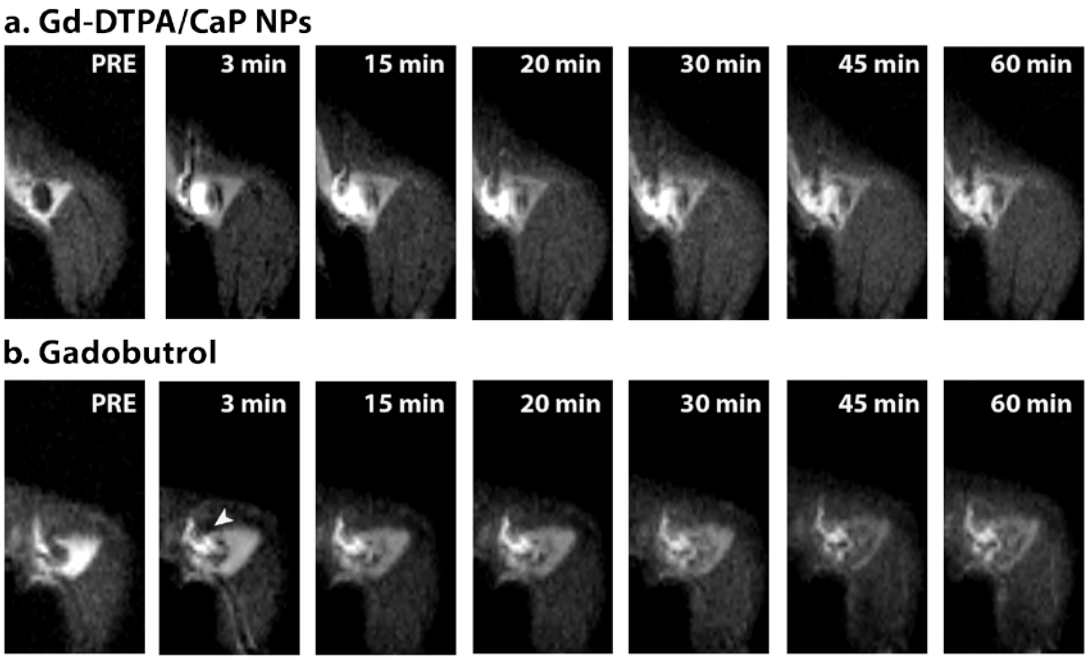


**Figure S12.** External compression of the injection site favours the uptake of the MRI tracer into the lymphatic vasculature. MRI images show the kinetics of Gd-DTPA/CaP NPs (a) or gadobutrol (b) deposition in the popliteal LN. Both Gd-DTPA/CaP NPs and gadobutrol quickly accumulated in the LN. Arrowheads point to regions of the LN where the increase in contrast enhancement can be first appreciated.

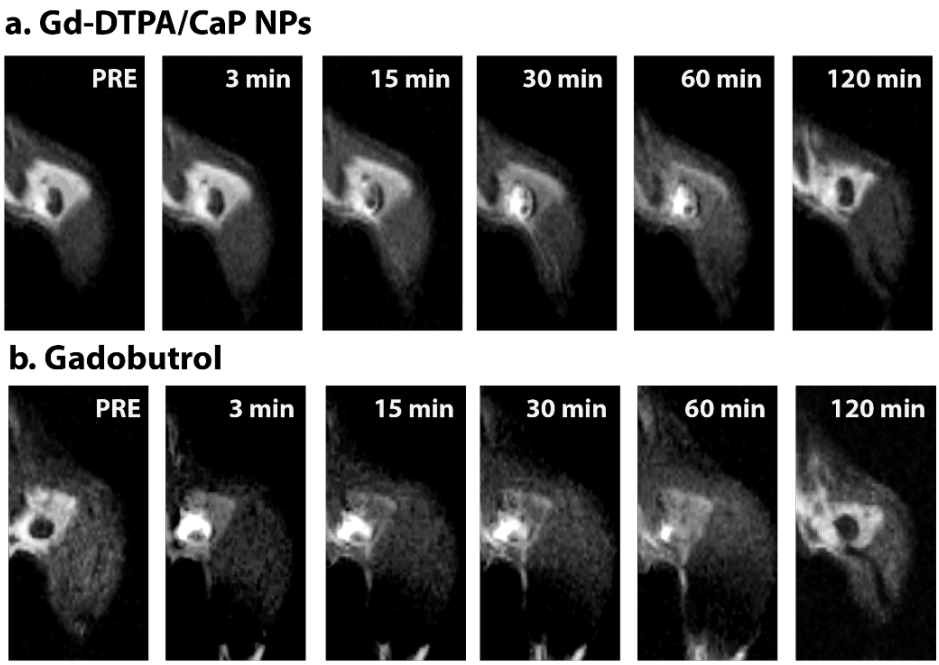


**Figure S13.** Precontrast and postcontrast MRI acquisitions of the left popliteal LN show that the contrast enhancement of Gd-DTPA/CaP NPs (a) and gadobutrol (b) fades away 120 min post administration of the tracers.